Inhibition Effect of 4-(2-Chlorophenyl)Hydrazineylidene-1-Phenyl-2-Pyrazolin-5-One Derivatives on Corrosion of 304 Stainless Steel in HCl Solution

Abd El-Aziz S. Fouda [1] , **Salah M. Rashwan** [2], **Medhat M. Kamel** [2], **Abdallah H.M. Gad** [2], **Kamal Shalabi** [1,*]

[1]   Department of Chemistry, Faculty of Science, El-Mansoura University, Egypt
[2]   Department of Chemistry, Faculty of Science, Suez Canal University, Egypt
*   Correspondence: dr-kamal@mans.edu.eg;

Abstract: 4-(2-chlorophenyl)hydrazineylidene-1-phenyl-2-pyrazolin-5-one derivatives (2-CPH) were examined as safe corrosion hindrance for 304 stainless steel (SS 304) in 1.0 M HCl utilizing weight loss (WL) and electrochemical tests such as potentiodynamic polarization (PP), electrochemical impedance spectroscopy (EIS) and electrochemical frequency modulation (EFM). The outcome data displayed that the protection efficiency (IE%) rises with improving the dose of 2-CPH compounds and lower with raising the temperature. The adsorption of these inhibitors on the surface of SS 304 follows Langmuir isotherm. The 2-CPH are the best inhibitors for the dissolution of SS 304 in 1M HCl and they are mixed kind inhibitors. Quantum calculations (QM) display the impact of the chemical structure of the 2-CPH on its %IE. Additionally, 304 stainless surface topography in one molar HCl solution without and with 2-CPH compounds appending utilizing atomic force microscopy (AFM) approves the protection of 304 stainless via adsorbed 2-CPH compounds by a formed protective layer.

Keywords: corrosion inhibition; 304 stainless; EIS; EFM; SEM; AFM.

1. Introduction

Stainless steel is a popular choice for the uses because best mechanical properties [1] and good dissolution resistance [2] SS is the main construction material, which is widely utilized in most of the main manufacturing. The corrosion hindrance of these metal alloys has been qualified to create an oxide film on the surface of SS [3, 4]. This time, it is a major training to utilized corrosion protectors to increase the dissolution resistance of 304 SS. Specifically, the corrosion hindrance of 304 SS in an acid environment with inhibitors is significant as the alloy often gets subjected to acids throughout procedures. The impact of numerous organic inhibitors in corrosion hindrance of 304 SS in the acid environment has been examined [5, 6]. Organic composites having N, O, S, or P atom (i.e., hetero-atoms), multiple bonds or aromatic systems which can be adsorbed on the superficial of alloy concluded lone pair of electrons and/or π-electrons are frequently verified to be remarkably effective inhibitors versus dissolution [7, 8]. Composites inclosing pyrazolinone moiety, are known to display diverse pharmacological activities [9-11].

In the current work, the impact of 2-CPH compounds as a safe inhibitor for the dissolution of 304 SS in 1M HCl was tested at altered temperatures. In this paper, the 2-CPH

compounds were utilized as inhibitors because 2-CPH compounds include multiple active centers, and they have a distinct affinity to protect SS 304 corrosion in HCl.

The inhibition proficiency of 2-CPH compounds for SS corrosion in 1 M HCl was estimated by WL, PP, EIS, and EFM. Finally, several methods have been used to study the inhibition behavior, including the theoretical and experimental data were matched.
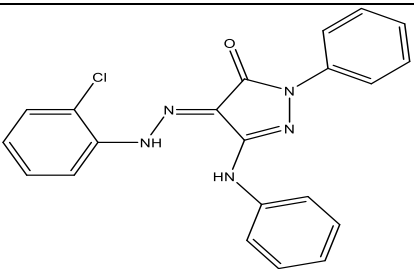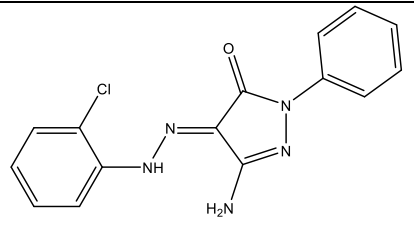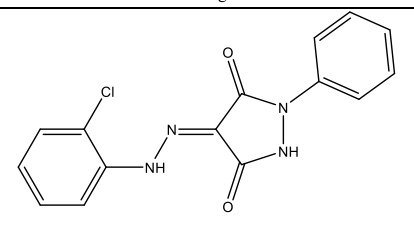
2. Materials and Methods

2.1. Materials and solutions.

The SS 304 specimens used for WL and electrochemical tests have the chemical conformation of (wt.%): 0.08 C, 0.75 Si, 18-20 Cr, 2.0 Mn, 10. 5 Ni, 0.045 P, and the rest Fe.

The examined 2-CPH compounds were produced, conferring to the techniques demonstrated in previously published papers [9-11]. These compounds are existing in Table 1. All preparation of the aggressive solution was done by utilizing distilled water to dilute analytical reagent grade 34% HCl to obtain the desired dose 1 M HCl. The stock solutions of 2-chlorophenyl hydrazine (2-CPH) derivatives 10^{-3} M were diluted with distilled to ready doses range from (4×10^{-6} – 24×10^{-6} M).

Table 1. The Chemical structure of 2-CPH derivatives.

Inhibitor	Structure
2-CPH1	(*E*)-4-(2-(2-chlorophenyl)hydrazineylidene)-2-phenyl-5-(phenylamino)-2,4-dihydro-3*H*-pyrazol-3-one Molecular Weight: 389.84
2-CPH2	(*E*)-5-amino-4-(2-(2-chlorophenyl)hydrazineylidene)-2-phenyl-2,4-dihydro-3*H*-pyrazol-3-one Molecular Weight: 313.75
2-CPH3	(*E*)-4-(2-(2-chlorophenyl)hydrazineylidene)-1-phenylpyrazolidine-3,5-dione Molecular Weight: 314.73

2.2. Corrosion inhibition evaluation.

2.2.1. WL test.

Samples of 304 stainless with a dimension of $2 \times 2 \times 0.2$ cm^2 were scratched with altered grades of emery papers from 400 to 1200 rinsed by doubled-distilled many times and dried. Consequently exact massed, the 304 SS sheets were put in a glass bottle (open system),

encloses 50 ml of HCl attendance, and lack adding an altered dose of 2-CPH compounds for 3 hrs. After every 30 min. the 304 SS were gotten, washed, dried, and massed prudently. The average WL (mg cm^{-2}) of the seven coins SS 304 should be obtained.

The grade of surface coverage (θ) and (IE %) of 2-CPH for SS 304 dissolution in 1 M HCl were measured from equation (1):

$$\%IE = \theta \times 100 = \left[1 - \frac{W}{W°}\right] \times 100 \qquad (1)$$

"where W^o and W are the values of the average WL without and with the addition of 2-CPH compounds, respectively."

2.2.2. Electrochemical tests.

All electrochemical measurements were applied into a three electrodes electrochemical cell including, the working electrode is SS 304, the reference electrode is Ag/AgCl, and the counter electrode is a platinum disk. Before each electrochemical test, the SS 304 electrode was immersed for 30 min in the solution to provide the possibility to the open circuit potential (OCP) to achieve a steady-state. Each experiment was achieved on a freshly abraded electrode utilizing a newly prepared electrolyte.

PP acquired by sweeping the electrode potential from -500 to 500 mV vs. (OCP), with a sweep rate of 1 mVs^{-1}. (IE%) and (θ) is measured from (i$_{corr}$) in equation (2).

$$\%IE = \theta \times 100 = \left[1 - \frac{i_{corr}}{i°_{corr}}\right] \times 100 \qquad (2)$$

"where $i°_{corr}$ and i_{corr} are corrosion current densities in the absence and existence of inhibitor, respectively".

EIS tests have executed in the experiment by applying AC signals range from (100 kHz to 0.1 Hz), with an amplitude of peaks 5mV at OCP. All the outcomes of impedance were agreeable with the suitable equivalent circuit employing the Gamry Echem program, and (IE%) and (θ) are measured by utilizing the charge transfer resistance (R$_{ct}$) as a function of the performance of protection.

$$\%IE = \theta \times 100 = \left[1 - \frac{R°_{ct}}{R_{ct}}\right] \times 100 \qquad (3)$$

"where R$^o_{ct}$ and R$_{ct}$ are the charge-transfer resistance values without and with inhibitor respectively"

EFM technique was achieved by relating two sine waves of 2 and 5 Hz [12, 13]. The parameters (i$_{corr}$), CF-2 and CF-3, and (βc and βa) have been measured [14]. (θ) and (%IE) are determine conferring to equation (2) like the PP.

All electrochemical techniques were executed using Potentiostate/Galvanostate (PCI4-G750) with Gamry framework software for measurements, linked to a PC for data documented and saved.

2.3. Surface analysis.

SS coins attendance and lack is dipping to 1 M HCl attendance and lack appending 24x10^{-6} M 2-CPH compounds for 24 hrs. , The surface morphology of 304 stainless coins was accepted by Pico SPM2100 for AFM analysis.

2.4. Quantum chemical calculations (QM).

QM calculations were realized utilizing Materials Studio style 7.0 from Accelrys Inc. USA [15-17]. DMol^3 model was utilized for QM by relating GGA technique with DNP origin set and BOP functional encloses COSMO controls [18-21].

3. Results and Discussion

3.1. WL tests.

The WL bends for SS 304 in mg cm^{-2} of the surface area dissolution in 1 M HCl existence and lack appending of altered doses of 2-CPH1 are displayed in Fig. 1 for 2-CPH1. The time-WL lines gotten in the attendance of 2-CPH1 are found under that of 1M HCl (blank). When the 2-CPH1 doses rise, WL is lowered, θ rises, and the %IE improves. %IE's are recorded in Table 2. This is initiated by the adsorption of 2-CPH on SS 304 surface producing a coating layer that separates the SS 304 from the aggressive environment and reduces the 304 stainless dissolutions. Therefore, the rate of dissolution reductions, with doses increases [22]. The order of %IE for 2-CPH compounds are determined from the calculated values of % IE is as the following:
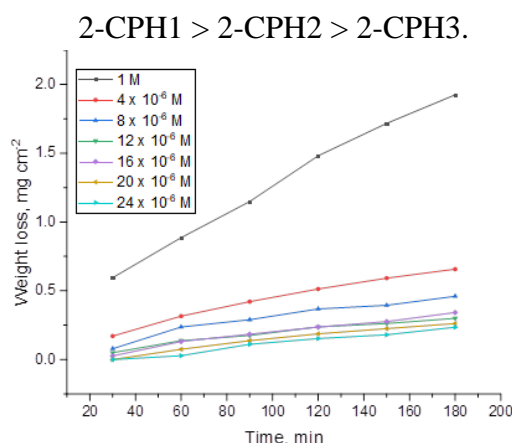
2-CPH1 > 2-CPH2 > 2-CPH3.

Figure 1. Time WL diagrams for SS 304 in 1 M HCl with and without various doses of 2-CPH1 at 30 ºC.

Table 2. The corrosion rate (C.R) and (%IE) for SS304 dipping in 1 M HCl and the existence of 2-CPH derivatives from WL tests at 30ºC.

Inhibitor	Conc. μM	C.R. mg cm^{-2}min^{-1}	θ	%IE
1 M HCl	0	0.0123	-	-
2-CPH1	4	0.0042	0.653	65.3
	8	0.003	0.751	75.1
	12	0.0019	0.839	83.9
	16	0.0019	0.84	84
	20	0.0015	0.873	87.3
	24	0.0012	0.897	89.7
2-CPH2	4	0.0046	0.626	62.6
	8	0.0031	0.742	74.2
	12	0.0026	0.786	78.6
	16	0.0025	0.794	79.4
	20	0.0019	0.839	83.9
	24	0.0014	0.881	88.1
2-CPH3	4	0.0041	0.662	66.2
	8	0.003	0.751	75.1
	12	0.002	0.831	83.1
	16	0.0024	0.804	80.4
	20	0.0018	0.848	84.8
	24	0.0017	0.859	85.9

3.2. Adsorption isotherm.

Several tests were made to fit the investigational data to altered isotherms. Altered adsorption isotherms were utilized to fit θ values to several isotherms counting Frumkin, Langmuir, Temkin, and Freundlich; it was found that the Langmuir isotherm is the most appropriate isotherm for our outcomes data and can be displayed by (Eq. 4) [23]:

$$\frac{C}{\theta} = \frac{1}{K_{ads}} + C \qquad (4)$$

"where C is the concentration (M) of the inhibitor in the bulk electrolyte, θ is the degree of surface coverage, K_{ads} is the adsorption equilibrium constant (M^{-1})"

For 2-CPH the linear regressions among C/θ and C are displayed in Fig. 2. The K_{ads} could be determined from the intercepts, and the standard free adsorption energy (ΔG^o_{ads}) can be computed from the K_{ads} values as follows [24]:

$$log\ K_{ads} = -log\ 5\ 5.5 - \frac{\Delta G^{°}_{ads}}{2.303RT} \qquad (5)$$

"where 55.5 is the molar concentration of water in the solution in mol/ L, R is the gas constant $(8.314\ J\ K^{-1}mol^{-1})$, T is the absolute temperature (K)"

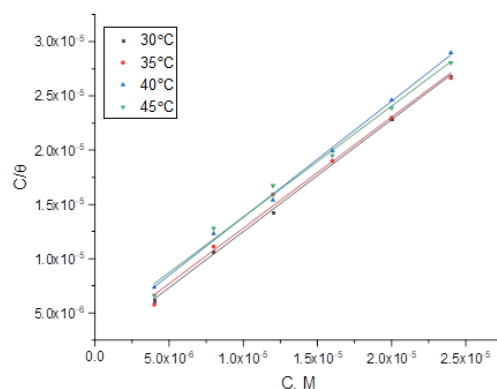**Figure 2**. Langmuir bends for the adsorption of 2-CPH1 on SS 304 in 1M HCl at various temperatures.
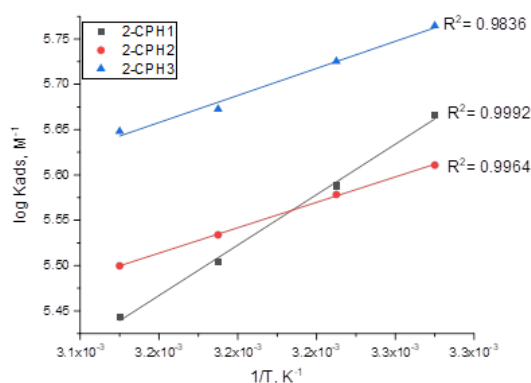

Figure 3. Plots of log K_{ads} vs. 1/ T for corrosion of SS 304 in 1 M HCl in the absence and existence of altered doses of 2-CPH derivatives.

The ΔG^o_{ads} data at all temperatures are listed in Table 3. The $(\Delta H^o_{ads.})$ was assessed based on the Van't Hoff equation.

$$log K ads = -\frac{\Delta H^{\circ}_{ads}}{2.303RT} + \text{constant} \qquad (6)$$

Table 3. The adsorption isotherm results for dissolution of SS 304 in 1 M HCl solution in the attendance of 2-CPH derivatives at altered temperature.

Inhibitor	Temp, °C	K x10³ M⁻¹	ΔG°ads kJ mol⁻¹	ΔH°ads	ΔS°ads
2-CPH1	30	463.336	-43.011	-27.74	50.392
	35	387.517	-43.263	-27.74	50.392
	40	319.462	-43.462	-27.74	50.224
	45	277.567	-43.785	-27.74	50.448
2-CPH2	30	408.308	-42.692	-14.19	94.068
	35	378.813	-43.205	-14.19	94.204
	40	341.979	-43.640	-14.19	94.089
	45	316.063	-44.128	-14.19	94.146
2-CPH3	30	581.550	-43.584	-14.85	94.818
	35	531.344	-44.072	-14.85	94.863
	40	470.566	-44.471	-14.85	94.622
	45	446.181	-45.040	-14.85	94.926

Plotting (log K_{ads}) vs. (1/T) gives a straight line as demonstrated in Fig. 3, the slope = (-ΔH°ads /2.303R), from this slope; the ΔH°ads data was measured and is arranged in Table 3. Then by applying the following equation [25]:

$$\Delta G^{\circ}_{ads} = \Delta H^{\circ}_{ads} - T\Delta S^{\circ}_{ads} \qquad (7)$$

The data present in Table 3 confirm the spontaneous adsorption of 2-CPH extricate on the 304 stainless surfaces, through the negative data obtained ΔG^{0}_{ads}, whose negative value (spontaneous) when negative values are greater than 40 kJ /mol, adsorption is chemical adsorption, representative the creation of coordinate bonds among an active site of 2-CPH (N, O, benzene ring) and empty d-orbitals of the iron [26, 27]. ΔH°ads had a negative sign for the 2-CPH display the adsorption of 2-CPH composite is an exothermic process. ΔS°ads had a positive sign for the 2-CPH with no noticeable variation at altered temperatures suggest that change at various temperatures indicate that 2-CPH molecules were adsorbed or accompanied by water molecules desorbed from the 304 stainless, which increases the randomness [28].

3.3. PP evaluation.

PP bends for SS 304 dissolution in 1 M HCl existence and lack altered 2-CPH1 doses at 25°C are demonstrated in Fig. 4. In which an electrochemical solution's potential is formed, and E_{corr} is measured, i_{corr} from the Tafel curve (i^{o}_{corr}), θ and IE% are reported in Table 4 [29, 30].

PP bends for 304 stainless in 1.0 M HCl, in the existence and lack of 2-CPH dose are displayed in Fig. 4. The parallel Tafel lines β_a & βc indicate that both anodic and cathodic mechanisms do not impact adding the 2-CPH to the corrosive environment. The data in Table 4 displays that the lower i_{corr} data in the existence of 2-CPH without affecting important exchanges in E_{corr} recommends that the 2-CPH is a mixed kind [31, 32]. %IE behaviors of the 2-CPH composite signify their affinity to lower both anodic reaction and cathodic of 304 SS in 1 M HCl by protected active centers [33]. The order of %IE for 2-CPH is: 2-CPH1 > 2-CPH2 > 2-CPH3, which agrees with obtained results from weight loss results.
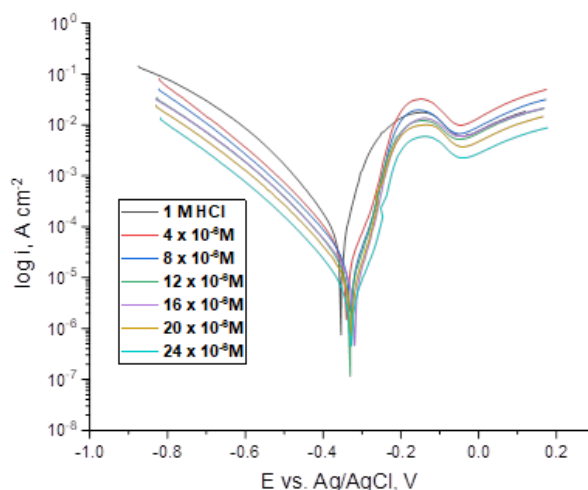
Figure 4. PP for SS 304 in 1 M HCl without and with various doses of 2-CPH1 at 25°C.

Table 4: Polarization results for SS 304 in 1 M HCl, including the altered dose of 2-CPH derivatives at 25°C.

Concentration, μM		i_{corr}, μAcm^{-2}	$-E_{corr}$, mV	b_a, mV/decade	$-b_c$, mV/decade	C.R., mpy	θ	%IE
1M HCl		71.10	354.0	46.3	105.7	32.47	--	--
2-CPH1	4	28.10	339.0	67.1	113.9	12.850	0.605	60.5
	8	19.70	329.0	57.1	121.6	8.988	0.723	72.3
	12	12.20	330.0	52.1	111.7	5.552	0.828	82.8
	16	10.40	320.0	51.2	111.7	4.764	0.854	85.4
	18	8.43	328.0	52.6	122.1	4.307	0.881	88.1
	20	5.27	328.0	64.2	119.7	2.406	0.926	92.6
2-CPH2	4	33.00	335.0	38.6	113.3	15.060	0.536	53.6
	8	23.70	331.0	34.3	109.7	9.446	0.667	66.7
	12	14.40	334.0	39.4	112.7	6.580	0.797	79.7
	16	12.50	332.0	42.0	121.1	5.722	0.824	82.4
	18	10.10	339.0	38.7	123.1	5.016	0.858	85.8
	20	7.14	342.0	39.3	115.8	2.803	0.900	90.0
2-CPH3	4	36.80	335.0	43.0	117.7	16.830	0.482	48.2
	8	26.30	336.0	41.6	128.2	12.000	0.630	63.0
	12	18.90	333.0	49.2	116.1	8.618	0.734	73.4
	16	14.8	327.0	33.4	119.6	5.863	0.792	79.2
	18	11.20	339.0	39.2	118.2	5.109	0.842	84.2
	20	8.65	321.0	33.3	122.9	3.947	0.878	87.8

3.4. Electrochemical impedance evaluation.

Figs. 5a, b displays the Nyquist and Bode diagrams for 304 stainless surface dipping at 1.0 M HCl lack and existence of altered 2-CHP1 doses at 25°C as the 2-CHP1 dose decreased, the diameter of the semicircle rises [34]. The deflection from the perfect semicircle normally owed to the dispersal of frequencies and the surface's inhomogeneity, grain boundaries, and impurities [35].

In Fig. 6, the equivalent circuit investigated the EIS spectra for 304 stainless dissolutions in 1 M HCl attendance and lack is appending 2-CPH. The equivalent circuit contained (R_{ct}), (R_s), and (CPE). The impedance Z_{CPE} can be assessed from the following equation (8) [36]:

$$Z_{CPE} = \frac{1}{Y_0(j\omega)^n} \qquad (9)$$

"where Y_0 is the admittance of the CPE, j is the imaginary number, ω is the angular frequency and n is the CPE exponent defined as phase shift".
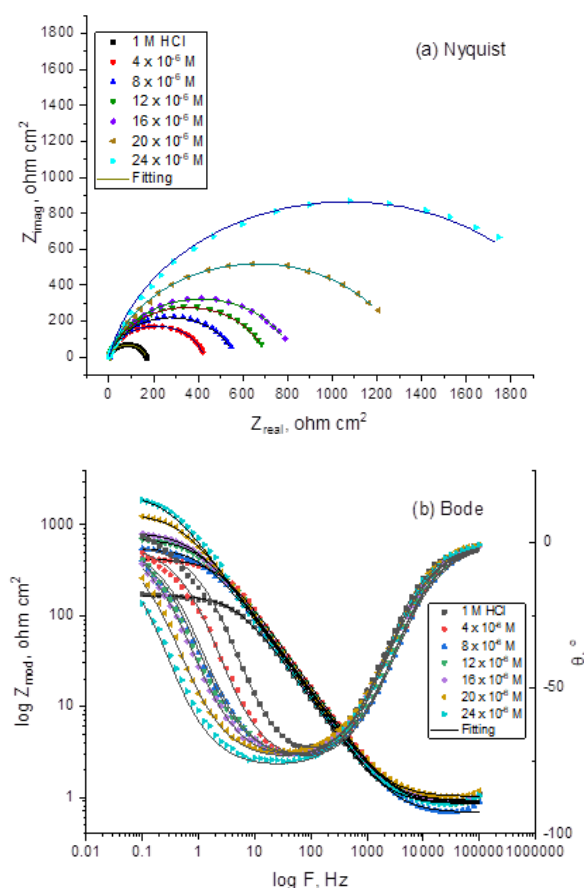
Figure 5. The Nyquist (a) and Bode (b) bends for SS 304 in 1 M HCl with and without of altered dose of 2-CPH1 at 25° C.
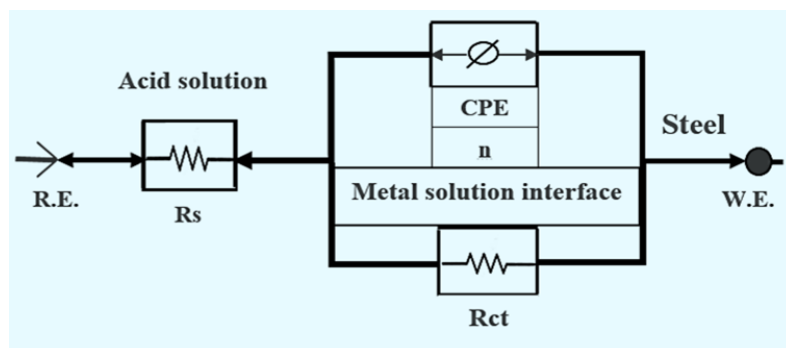

Figure 6. Equivalent electrical circuit utilized to fit the impedance data.

The data of n exponent (Table 5) show an exchange from 0.782 to 0.872 representative non-ideal capacitive behavior, which assigned to the heterogeneity of 304 stainless surfaces remaining to the surface roughness [36, 37].

Table 5 reported the EIS parameters. Increasing the doses of the 2-CPH raises the (R_{ct}) owing to the rises in the thickness of the adsorbed layer and lower the (C_{dl}), as a result of the thickness rising of the electrical double layer or/and the lesser in the dielectric constant due to the substitution of the adsorbed water molecules on 304 stainless by the 2-CPH molecules, recommends that the 2-CPH molecules function by adsorption at the 304SS/interface [38]. The order of %IE for 2-CPH is: 2-CPH1 > 2-CPH2 > 2-CPH3, which agrees with obtained results from WL and PP results.

Table 5. EIS parameters for SS 304 in 1 M HCl in the attendance and lack altered dose of 2-CPH derivatives at 25°C.

concentration, μM		$R_s,$ ohm cm^2	$R_{ct},$ kohm cm^2	$Y_0,$ μohm s^n cm^{-2}	n	$C_{dl},$ μFcm^{-2}	Θ	%IE
blank		0.88	165.60	382.70	0.872	254.90	--	--
2-CPH1	4	0.90	423.70	323.30	0.869	239.84	0.609	60.9
	8	0.86	556.40	315.70	0.852	233.27	0.702	70.2
	12	0.84	702.90	285.90	0.847	213.86	0.764	76.4
	16	0.92	822.30	274.50	0.848	210.26	0.799	79.9
	20	1.02	1326.00	256.79	0.826	204.78	0.875	87.5
	24	0.85	2129.00	237.50	0.811	202.62	0.922	92.2
2-CPH2	4	0.62	395.50	325.80	0.865	236.82	0.581	58.1
	8	0.69	484.00	312.90	0.863	231.88	0.658	65.8
	12	0.80	597.00	306.34	0.836	219.51	0.723	72.3
	16	0.86	782.10	278.20	0.854	214.35	0.788	78.8
	20	0.74	1136.00	263.00	0.843	209.94	0.854	85.4
	24	0.70	1649.00	249.32	0.831	208.20	0.900	90.0
2-CPH3	4	0.62	355.40	330.50	0.843	221.93	0.534	53.4
	8	0.85	415.60	252.40	0.847	167.69	0.602	60.2
	12	0.90	530.10	242.20	0.840	163.63	0.688	68.8
	16	0.69	688.60	239.00	0.817	159.63	0.760	76.0
	20	0.73	990.80	226.30	0.805	157.69	0.833	83.3
	24	0.83	1347.00	218.46	0.782	155.37	0.877	87.7

3.5. Electrochemical frequency modulation (EFM).

EFM technology is fast and not destructive. i_{corr}, causal factors CF2 and CF3, and Tafel slopes (β_a and β_c) were determined through the higher peaks. The data obtained from EFM for 304 stainless 1 M HCl with an altered dose of 2-CPH at 25 °C were assessed and are recorded in Table 6.
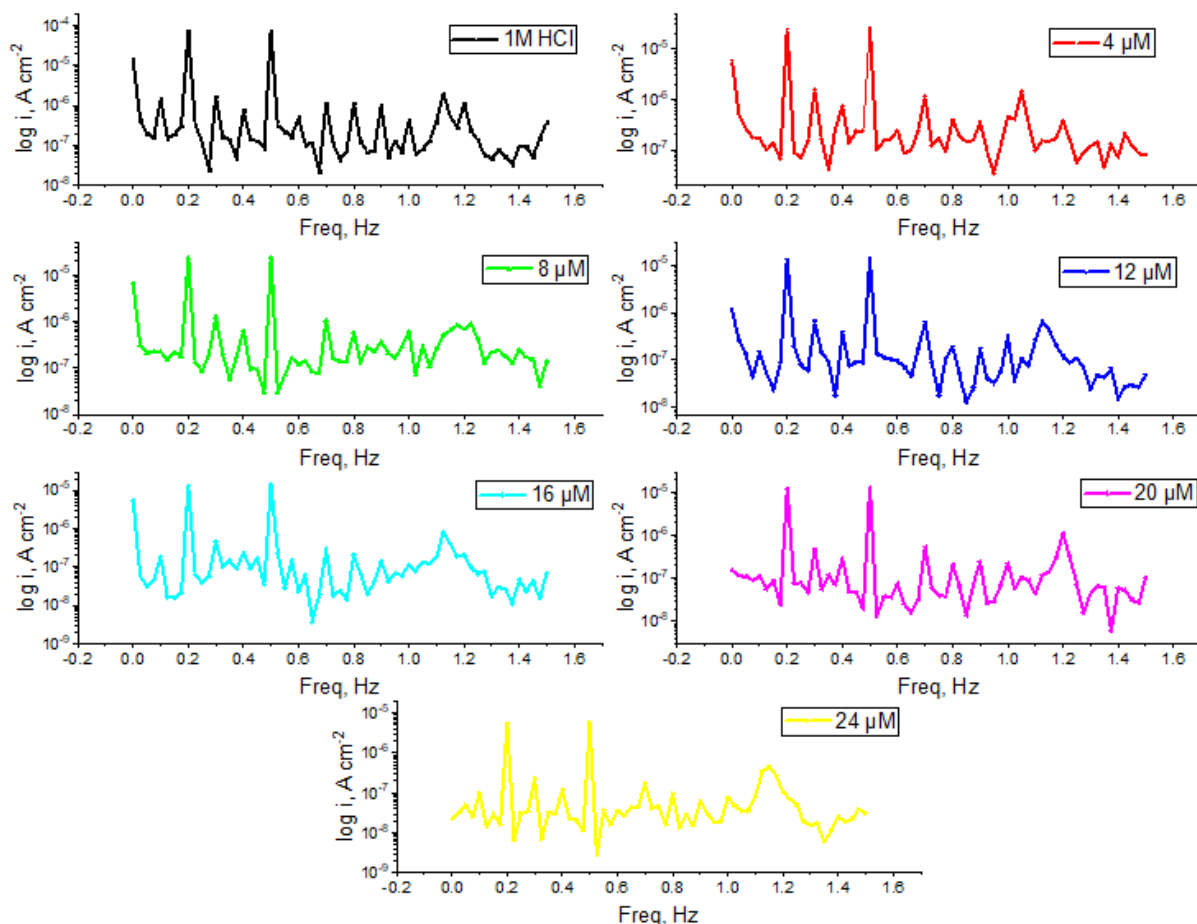

Figure 7. EFM graphs for SS 304 in 1 M HCl with and without various concentrations of 2-CPH1 at 25°C.

The data detected that i_{corr} lowered by improving the dose of 2-CPH while the IE% raises. The CF (causality factor) is close to their theoretical data [39, 40]. The IE% can be calculated as in Eq. 2. The spectra achieved from EFM in lack and attendance of altered dose of 2-CPH1 are displayed in Fig. 7. EFM data are in excellent agreement with the outcome data attained through other electrochemical tests. The order of inhibition proficiency for 2-CPH compounds is 2-CPH1 > 2-CPH2 > 2-CPH3, which agrees with obtained results from WL, PP, and EIS results.

Table 6. Electrochemical parameters were obtained from EFM technique for SS 304 in 1 M HCl without and with different concentrations of 2-CPH derivatives at 25°C.

	Concentration, mM	i_{corr}, μAcm^{-2}	b_a, mV/decade	$-b_c$, mV/decade	C.R., mpy	CF-2	CF-3	q	IE
	blank	98.04	85.1	94.9	44.77	2.417	2.67	--	--
2-CPH1	4	39.80	89.5	127.8	18.190	2.255	2.000	0.594	59.4
	8	30.48	74.4	96.0	13.920	1.850	3.556	0.689	68.9
	12	22.65	95.3	131.9	10.340	1.814	2.820	0.769	76.9
	16	20.00	90.6	107.8	9.131	2.138	3.945	0.796	79.6
	18	11.99	58.7	68.7	5.474	1.963	4.695	0.878	87.8
	20	7.95	83.4	102.5	3.631	2.089	2.677	0.919	91.9
2-CPH2	4	41.68	80.1	99.9	19.030	2.427	3.038	0.575	57.5
	8	33.19	78.0	95.4	15.150	1.764	4.254	0.661	66.1
	12	25.18	81.2	99.2	11.500	1.429	2.308	0.743	74.3
	16	21.24	88.7	113.0	9.700	1.719	2.219	0.783	78.3
	18	14.00	79.0	104.9	6.391	1.727	2.930	0.857	85.7
	20	9.79	82.5	114.5	4.472	1.442	3.380	0.900	90.0
2-CPH3	4	44.82	80.1	99.9	20.460	2.138	3.025	0.543	54.3
	8	37.73	67.7	136.2	17.230	2.054	2.790	0.615	61.5
	12	29.99	83.2	109.7	13.690	1.839	2.820	0.694	69.4
	16	24.94	71.3	119.1	11.390	1.884	2.962	0.746	74.6
	18	17.76	79.2	105.3	8.111	1.729	2.913	0.819	81.9
	20	12.96	72.7	96.3	5.919	1.857	2.872	0.868	86.8

3.6. Surface analysis.

Fig. 8a-e displays the 2D and 3D AFM morphology for the 304 stainless surfaces earlier and later sinking in 1 M HCl in the lack and existence of 24×10^{-6} M of 2-CPH compounds. Fig. 8a display AFM polished 304 stainless surfaces (bare metal) seems smooth, with little roughness (28.22 nm). After dipping in HCl (blank) for 24 hrs., dissolution happens, the roughness of 304 stainless rises (382.86 nm) as exposed in Fig. 8b. After 24 hrs. of dissolution, no pitting was detected on the 304 stainless in the attendance of 24×10^{-6} M of 2-CPH, and the roughness of surface reduced (115.31, 125.81, 137.22 nm) paralleled with the blank sample as exposed in Fig. 8c-e. The 304 stainless coins are smoothed by the adsorbed surface layers of the 2-CHP on the surface [41].

3.7. Quantum chemical calculations (QM).

The design of the relationship among the molecular structure of 2-CPH and its protective action gotten from QM. Table 7 demonstrations quantum chemical parameters measured for 2-CPH molecules, particularly E_{LUMO}, E_{HOMO}, the ΔE, and μ. Fig. 9 exhibitions optimized structure, HOMO, and LUMO for 2-CPH molecules.

The HOMO of 2-CPH molecules is mostly sited on N, O, and phenyl pyrazolidine moiety, which aids electron-donating from 2-CPH molecules to the 304 stainless (Fig. 9). 2-CPH1 has the highest E_{HOMO}, subsequently, the best corrosion inhibition action was for 2-CPH1 (-4.522eV) compared with 2-CPH2 (-4.657 eV) and 2-CPH3 (-4.944 eV).
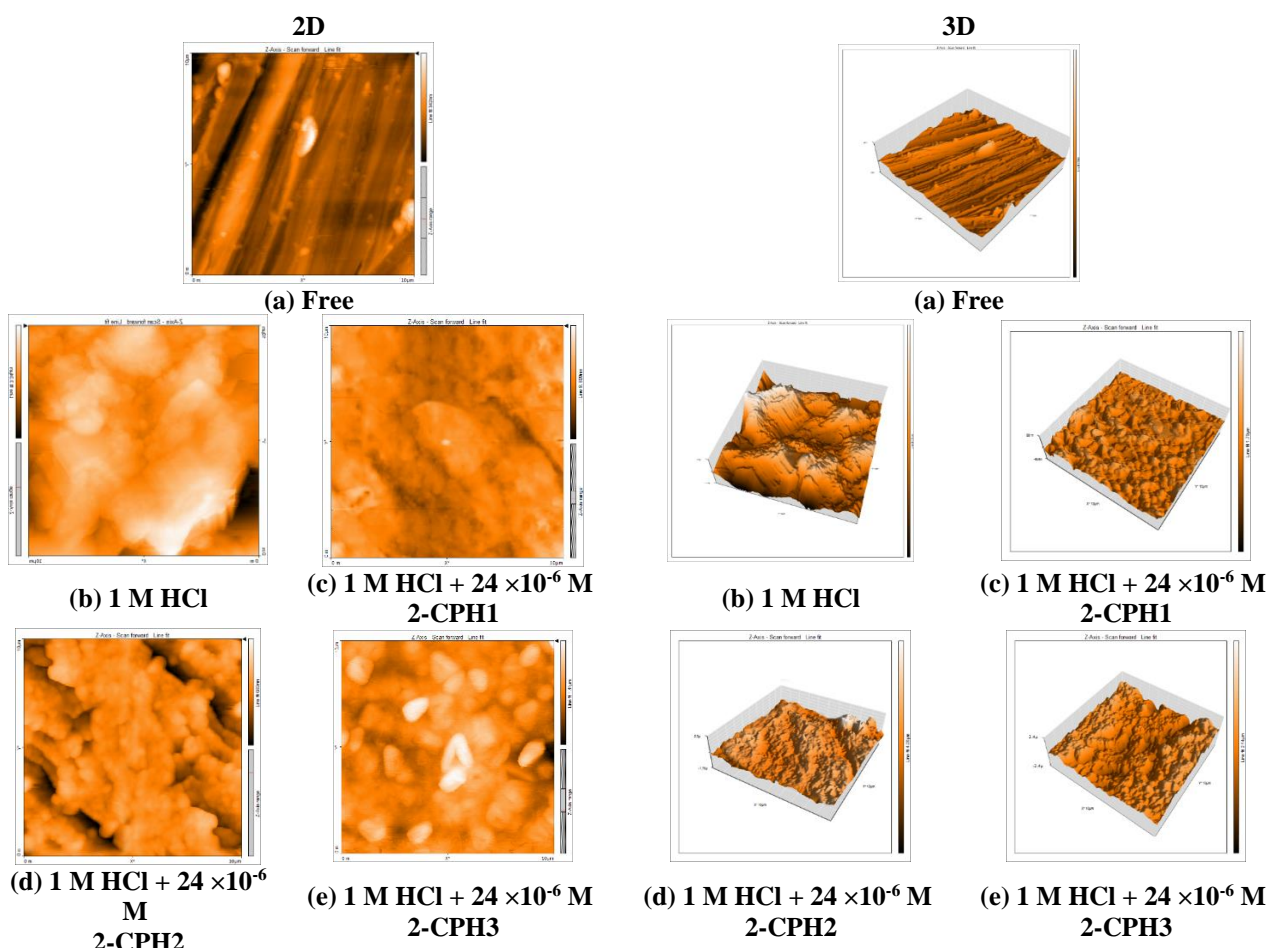
2D

(a) Free

3D

(a) Free

(b) 1 M HCl

(c) 1 M HCl + 24 ×10^{-6} M 2-CPH1

(b) 1 M HCl

(c) 1 M HCl + 24 ×10^{-6} M 2-CPH1

(d) 1 M HCl + 24 ×10^{-6} M 2-CPH2

(e) 1 M HCl + 24 ×10^{-6} M 2-CPH3

(d) 1 M HCl + 24 ×10^{-6} M 2-CPH2

(e) 1 M HCl + 24 ×10^{-6} M 2-CPH3

Figure 8. 2D and 3D AFM images of the surface of SS 304 (a) before exposure in 1 M HCl solution, (b) after immersion in 1 M HCl for 24 hr, and (c-e) after immersion in 1 M HCl in addition to 24 ×10^{-6} M of 2-CPH derivatives 24 hr at 25°C.
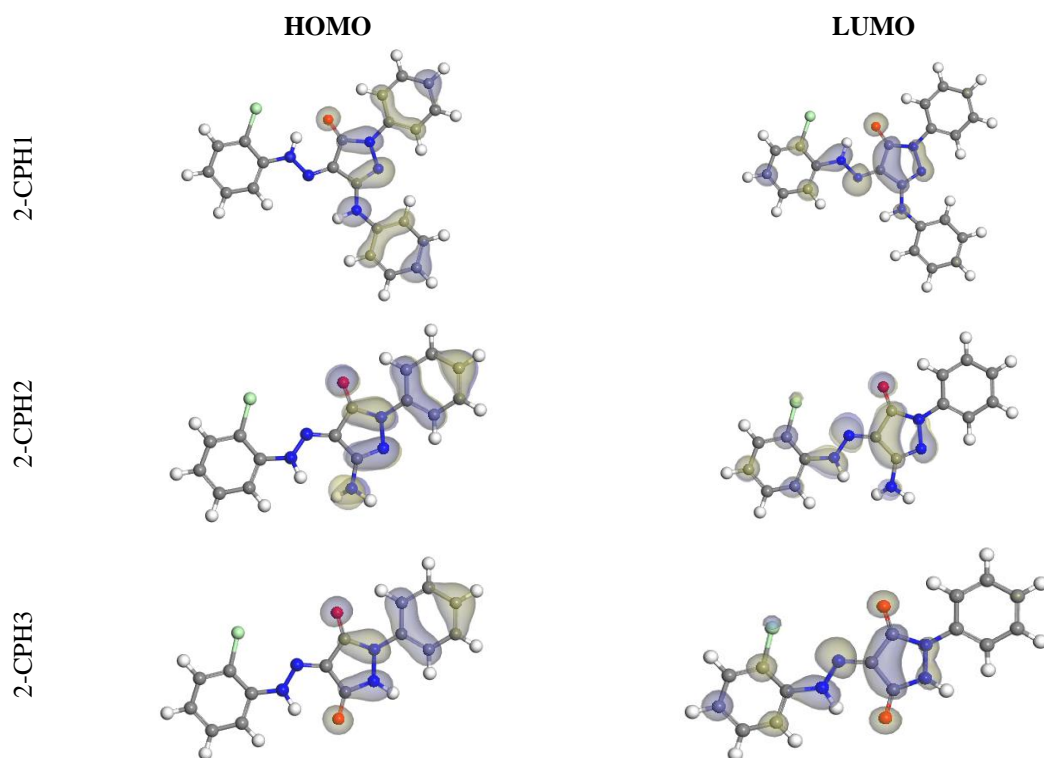
HOMO

LUMO

Figure 9. The HOMO and LUMO of the 2-CPH molecules using DMol^3.

Generally, the little data of the ΔE, the more simple to offer more electrons and excellent adsorption on 304 stainless surfaces [42]. Therefore, the lowest ΔE value for 2-CPH1 molecule (1.497 eV) realizes the adsorption and improves the %IE (Table 7).

Table 7 demonstrates the highest dipole moment for 2-CPH1 molecule (9.317 debye), which exposes an IE rises [43-45]. Additionally, the 2-CPH1 molecule has the highest surface area (393.217 $Å^2$), which raises the interaction area among the 2-CPH1 molecule and surface of 304 stainless or increment the area of 304 stainless coated with a molecule.

Table 7. The calculated quantum chemical parameters for 2-CPH derivatives utilizing $DMol^3$.

	2-CPH1	2-CPH2	2-CPH3
E_{HOMO}, eV	-4.522	-4.657	-4.944
E_{LUMO}, eV	-3.025	-2.941	-2.852
$DE = E_{LUMO} - E_{HOMO}$, eV	1.497	1.716	2.092
Dipole moment, debye	9.317	8.958	5.370
Molecular surface area, $Å^2$	393.217	320.823	314.136

3.8. Mechanism of inhibition.

According to the test examination, methods have been used to study the inhibition behavior, including the theoretical and the chemical structure of 2-CPH molecules, the protection mechanism of 2-CPH could be recommended. The examined 2-CPH molecules in an acidic medium can be dissociated into cation (protonated form). The protonated 2-CPH molecules have various active centers, which are the N, O atoms and p-orbitals of benzene [46]. Hence, "the hindrance of the 2-CPH may be achieved by the contribution of two methods of interaction: (a) Electrostatic attraction (physical adsorption) among the protonated 2-CPH particles (positive sign charge) and the cathodic destinations of SS surface (negative sign charge). Furthermore, an electrostatic association among the Cl-particle (negative sign charge), and the anodic destinations of SS surface (positive charge), (b) Chemical attraction (chemisorption) among the N^+ molecule and p-orbitals of benzene rings also, unpaired electrons of N, O atoms, and the vacant d-orbitals of iron surface molecules. In this way, using multiple sites of adsorptions, 2-CPH molecules can adhere strongly on 304 stainless surface" [46]. These methods of association were proportionate with the estimations of $\Delta G°_{ads}$, where the adsorption of 2-CPH is chemisorption.

4. Conclusions

From investigational and theoretical outcomes, we can assume that the 2-CPH derivatives are an excellent inhibitor to protect 304 stainless versus liquefaction in an acidic environment. Furtheremore, the %IE of 2-CPH derivatives raises with dose improving and the 2-CPH molecules adsorbed on the surface of 304 stainless were accepted by dropping the data of C_{dl} matching with a blank solution when the 2-CPH derivatives are existence and also confirmed by AFM tests. Morever, the adsorption of the 2-CPH derivatives on the 304 stainless in 1M HCl is assumed as chemisorption and described by Langmuir isotherm. Finally, the %IE for 304 stainless surfaces utilizing 2-CPH derivatives in 1 M HCl approved by both experimental and theoretical tests.

Funding

Acknowledgments

Conflicts of Interest

The authors declare no conflict of interest.

References

1. Shabani-Nooshabadi, M.; Ghandchi, M.-S. Introducing the Santolina chamaecyparissus Extract as a Suitable Green Inhibitor for 304 Stainless Steel Corrosion in Strong Acidic Medium. *Metallurgical and Materials Transactions A* **2015**, *46*, 5139-5148, https://doi.org/10.1007/s11661-015-3101-3.
2. Leiva-García, R.; Akid, R.; Greenfield, D.; Gittens, J.; Muñoz-Portero, M.J.; García-Antón, J. Study of the sensitisation of a highly alloyed austenitic stainless steel, Alloy 926 (UNS N08926), by means of scanning electrochemical microscopy. *Electrochimica Acta* **2012**, *70*, 105-111, https://doi.org/10.1016/j.electacta.2012.03.036.
3. Pardo, A.; Merino, M.C.; Coy, A.E.; Viejo, F.; Arrabal, R.; Matykina, E. Effect of Mo and Mn additions on the corrosion behaviour of AISI 304 and 316 stainless steels in H2SO4. *Corrosion Science* **2008**, *50*, 780-794, https://doi.org/10.1016/j.corsci.2007.11.004.
4. Düdükcü, M.; Yazici, B.; Erbil, M. The effect of indole on the corrosion behaviour of stainless steel. *Materials Chemistry and Physics* **2004**, *87*, 138-141, https://doi.org/10.1016/j.matchemphys.2004.05.043.
5. Goudarzi, N.; Peikari, M.; Reza Zahri, M.; Reza Mousavi, H. Adsorption and corrosion inhibition behavior of stainless steel 316 by aliphatic amine compounds in acidic solution. *Archives of Metallurgy and Materials* **2012**, *57,* 845-851, https://doi.org/10.2478/v10172-012-0044-1.
6. Goudarzi, N.; Farahani, H. Investigation on 2-mercaptobenzothiazole behavior as corrosion inhibitor for 316-stainless steel in acidic media. *Anti-Corrosion Methods and Materials* **2014**, *61*, 20-26, https://doi.org/10.1108/ACMM-11-2012-1223.
7. Saha, S.K.; Dutta, A.; Ghosh, P.; Sukul, D.; Banerjee, P. Novel Schiff-base molecules as efficient corrosion inhibitors for mild steel surface in 1 M HCl medium: experimental and theoretical approach. *Phys. Chem. Chem. Phys.* **2016**, *18*, 17898–911, https://doi.org/10.1039/C6CP01993E.
8. Olasunkanmi, L.O.; Ebenso, E.E. Experimental and computational studies on propanone derivatives of quinoxalin-6- yl-4,5-dihydropyrazole as inhibitors of mild steel corrosion in hydrochloric acid. *Journal of Colloid and Interface Science* **2020**, *561*, 104–116, https://doi.org/10.1016/j.jcis.2019.11.097.
9. Etman, H.A.; Sadek, E.G.; Metwally, M.A. New route for the synthesis of 3-anilino-4-aryl-hydrazono-1-phenyl-2-pyrazolin-5-ones. *Archives of Pharmacal Research* **1994**, *17*, 36-38, https://doi.org/10.1007/BF02978245.
10. Venkataramana, P.; Suryanarayana, B.S.; Ravindranath, L.K.; Seshagir, V. Electrochemical Behaviour of 1-Phenyl-3-Amino-4-(Substituted Benzeneazo)-Pyrazolin-5-ones in N, N'-Dimethylformamide. *Proceedings of the Indian National Science Academy, Part A: Physical Sciences* **1992**, *58*, 375-382.
11. Ramana, P.V.; Suryanarayana, B.S.; Ravindranath, L.K.; Rao, S.B.; Ramadas, S.R. Electrochemical behavior of 3-amino-1-phenyl-4-substituted benzene-azo) pyrazolin-5ones. *Indian Journal of Chemistry, Section A: Inorganic, Physical, Theoretical & Analytical* **1990**, *29,* 864-866.
12. Khaled, K.F. Evaluation of electrochemical frequency modulation as a new technique for monitoring corrosion and corrosion inhibition of carbon steel in perchloric acid using hydrazine carbodithioic acid derivatives. *Journal of Applied Electrochemistry* **2009**, *39*, 429-438, https://doi.org/10.1007/s10800-008-9688-y.
13. Li, W.; Zhang, Z.; Zhai, Y.; Ruan, L.; Zhang, W.; Wu, L. Electrochemical and Computational Studies of Proline and Captopril as Corrosion Inhibitors on Carbon Steel in a Phase Change Material Solution. *Int. J. Electrochem. Sci.* **2020**, *15*, 722–739**,** https://doi.org/10.20964/2019.01.50.
14. Lavanya, D.K.; Priya, F.V.; Vijaya, D.P. Green Approach to Corrosion Inhibition of Mild Steel in Hydrochloric Acid by 1-[Morpholin-4-yl(thiophen-2-yl)methyl]thiourea. *Journal of Failure Analysis and Prevention* **2020**, *20*, 494-502, https://doi.org/10.1007/s11668-020-00850-9.
15. Abdallah, Y.M.; Shalabi, K.; Bayoumy, N.M. Eco-friendly synthesis, biological activity and evaluation of some new pyridopyrimidinone derivatives as corrosion inhibitors for API 5L X52 carbon steel in 5% sulfamic acid medium. *Journal of Molecular Structure* **2018**, *1171*, 658-671, https://doi.org/10.1016/j.molstruc.2018.06.045.

16. Fouda, A.S.; El-Awady, G.Y.; El Behairy, W.T. Prosopis juliflora Plant Extract as Potential Corrosion Inhibitor for Low-Carbon Steel in 1 M HCl Solution. *Journal of Bio- and Tribo-Corrosion* **2017**, *4*, https://doi.org/10.1007/s40735-017-0124-x.

17. Rehim, S.S.A.; Hazzazi, O.A.; Amin, M.A.; Khaled, K.F. On the corrosion inhibition of low carbon steel in concentrated sulphuric acid solutions. Part I: Chemical and electrochemical (AC and DC) studies. *Corrosion Science* **2008**, *50*, 2258-2271, https://doi.org/10.1016/j.corsci.2008.06.005.

18. Fouda, A.S.; Abd El-Maksoud, S.A.; El-Hossiany, A.; Ibrahim, A. Corrosion Protection of Stainless Steel 201 in Acidic Media using Novel Hydrazine Derivatives as Corrosion Inhibitors. *Int. J. Electrochem. Sci.* **2019,** *14,* 2187-2207, https://doi.org/10.20964/2019.03.15.

19. Shimizu, K.; Lasia, A.; Boily, J.-F. Electrochemical Impedance Study of the Hematite/Water Interface. *Langmuir* **2012**, *28*, 7914-7920,https://doi.org/10.1021/la300829c.

20. Bosch, R.W.; Hubrecht, J.; Bogaerts, W.F.; Syrett, B.C. Electrochemical Frequency Modulation: A New Electrochemical Technique for Online Corrosion Monitoring. *Corrosion* **2001**, *57*, 60-70, https://doi.org/10.5006/1.3290331.

21. El-Askalany, A.H.; Mostafa,S. I.; Shalabi, K.; Eid, A.M.; Shaabana, S. Novel tetrazole-based symmetrical diselenides as corrosion inhibitors for N80 carbon steel in 1 M HCl solutions: Experimental and theoretical studies. *J. Mol. Liq.* **2016**, 223, 497-508, https://doi.org/10.1016/j.molliq.2016.08.088.

22. Fouda, A.S.; Abdel Azeem, M.; Mohamed, S.A., El-Hossiany, A.; El-Desouky, E. Corrosion Inhibition and Adsorption Behavior of Nerium Oleander Extract on Carbon Steel in Hydrochloric Acid Solution. *Int. J. Electrochem. Sci.* **2019,** *14,* 3932 – 3948, https://doi.org/10.20964/2019.04.44.

23. Bentiss, F.; Bouanis, M.; Mernari, B.; Traisnel, M.; Vezin, H.; Lagrenée, M. Understanding the adsorption of 4H-1,2,4-triazole derivatives on mild steel surface in molar hydrochloric acid. *Applied Surface Science* **2007**, *253*, 3696-3704, https://doi.org/10.1016/j.apsusc.2006.08.001.

24. Elkadi, L.; Mernari, B.; Traisnel, M.; Bentiss, F.; Lagrenée, M. The inhibition action of 3,6-bis(2-methoxyphenyl)-1,2-dihydro-1,2,4,5-tetrazine on the corrosion of mild steel in acidic media. *Corrosion Science* **2000**, *42*, 703-719, https://doi.org/10.1016/S0010-938X(99)00101-8.

25. Singh, A.K.; Quraishi, M.A. Investigation of the effect of disulfiram on corrosion of mild steel in hydrochloric acid solution. *Corrosion Science* **2011**, *53*, 1288-1297, https://doi.org/10.1016/j.corsci.2011.01.002.

26. Fouda, A.S.; Rashwan, S.; El-Hossiany, A.; El-Morsy, F.E. Corrosion Inhibition of Zinc in Hydrochloric Acid Solution using some organic compounds as Eco-friendly Inhibitors. *Journal of Chemical, Biological and Physical Sciences* **2019,** *9*, 001-024, https://doi.org/10.24214/jcbps.A.9.1.00124.

27. Sorkhabi, H.A.; Shaabani, B.; Seifzadeh, D. Corrosion inhibition of mild steel by some Schiff base compounds in hydrochloric acid. *App. Surf. Sci.* **2005**, *239*, 154-164, https://doi.org/10.1016/j.apsusc.2004.05.143.

28. Hsissou, R.; Abbout, S.; Berisha, A.; Berradi, M.; Assouag, M.; Hajjaji, N.; Elharfi, A. Experimental, DFT and molecular dynamics simulation on the inhibition performance of the DGDCBA epoxy polymer against the corrosion of the E24 carbon steel in 1.0 M HCl solution. *Journal of Molecular Structure* **2019**, *1182*, 340-351, https://doi.org/10.1016/j.molstruc.2018.12.030.

29. Arivazhagan, M.; Subhasini, V.P. Quantum chemical studies on structure of 2-amino-5-nitropyrimidine. *Spectrochim. Acta*. **2012**, *91*, 402-410, https://doi.org/10.1016/j.saa.2012.02.018.

30. Fouda, A.S.; Abd El-Maksoud, S.A.; El-Hossiany, A.; Ibrahim, A. Effectiveness of Some Organic Compounds as Corrosion Inhibitors for Stainless Steel 201 in 1M HCl: Experimental and Theoretical Studies. *Int. J. Electrochem. Sci.* **2018,** *13*, 9826–9846, https://doi.org/10.20964/2018.10.36.

31. Prabhu, R.A.; Venkatesha, T.V.; Shanbhag, A.V.; Kulkarni, G.M.; Kalkhambkar, R.G. Inhibition effects of some Schiff's bases on the corrosion of mild steel in hydrochloric acid solution. *Corrosion Science* **2008**, *50*, 3356-3362, https://doi.org/10.1016/j.corsci.2008.09.009.

32. Shainy, K.M.; Rugmini Ammal, P.; Unni, K.N.; Benjamin, S.; Joseph, A. Surface Interaction and Corrosion Inhibition of Mild Steel in Hydrochloric Acid Using Pyoverdine, an Eco-Friendly Bio-molecule. *Journal of Bio- and Tribo-Corrosion* **2016**, *2*, https://doi.org/10.1007/s40735-016-0050-3.

33. El-Sayed, A.-R.; Mohran, H.S.; Abd El-Lateef, H.M. The inhibition effect of 2,4,6-tris (2-pyridyl)-1,3,5-triazine on corrosion of tin, indium and tin–indium alloys in hydrochloric acid solution. *Corrosion Science* **2010**, *52*, 1976-1984, https://doi.org/10.1016/j.corsci.2010.02.029.

34. Fouda, A.S.; Abd El-Maksoud, S.A.; El-Hossiany, A.; Ibrahim, A. Evolution of the Corrosion-inhibiting Efficiency of Novel Hydrazine Derivatives against Corrosion of Stainless Steel 201 in Acidic Medium. *Int. J. Electrochem. Sci.* **2019,** *14*, 6045–6064, https://doi.org/10.20964/2019.07.65.

35. Bidi, M.A.; Azadi, M.; Rassouli, M. A new green inhibitor for lowering the corrosion rate of carbon steel in 1 M HCl solution: Hyalomma tick extract. *Materials Today Communications* **2020**, *24*, 1-9, https://doi.org/10.1016/j.mtcomm.2020.100996.

36. Hou, B.S.; Zhang, Q.H.; Li, Y.Y.; Zhu, G.Y.; Liu, H.F.; Zhang, G.A. A pyrimidine derivative as a high efficiency inhibitor for the corrosion of carbon steel in oilfield produced water under supercritical CO2 conditions. *Corros. Sci.* **2020**, *164*, 1-18, https://doi.org/10.1016/j.corsci.2019.108334.

37.   Gopi, D.; Govindaraju, K.M.; Kavitha, L. Investigation of triazole steel derived Schiff bases as corrosion inhibitors for mild steel in hydrochloric acid medium. *J. Appl. Electrochem.* **2010**, *40*, 1349-1355, https://doi.org/10.1007/s10800-010-0092-z.

38.   Motawea, M. M.; El-Hossiany, A.; Fouda, A.S. Corrosion Control of Copper in Nitric Acid Solution using Chenopodium Extract. *Int. J. Electrochem. Sci.* **2019,** *14*, 1372–1387, https://doi.org/10.20964/2019.02.29.

39.   Emori, W.; Zhang, R.H.; Okafor, P.C.; Zheng, X.W.; He, T.; Wei, K.; Lin, X.Z.; Cheng, C.R. Adsorption and corrosion inhibition performance of multi-phytoconstituents from Dioscorea septemloba on carbon steel in acidic media: Characterization, experimental and theoretical studies. *Colloids and Surfaces A: Physicochemical and Engineering Aspects.* **2020**, *590*, 1-13, https://doi.org/10.1016/j.colsurfa.2020.124534.

40.   Fouda, A.S.; Eissa, M.; El-Hossiany, A. Ciprofloxacin as Eco-Friendly Corrosion Inhibitor for Carbon Steel in Hydrochloric Acid Solution. *Int. J. Electrochem. Sci.* **2018,** *13*, 11096–11112, https://doi.org/10.20964/2018.11.86.

41.   Li, Y.; Cheng, Y.F. Effect of surface finishing on early-stage corrosion of a carbon steel studied by electrochemical and atomic force microscope characterizations. *Appl. Surf. Sci.* **2016**, *366,* 95-103, https://doi.org/10.1016/j.apsusc.2016.01.081.

42.   Baymou, Y.; Bidi, H.; Ebn Touhami, M.; Allam, M.; Rkayae, M.; Belakhmima, R.A. Corrosion Protection for Cast Iron in Sulfamic Acid Solutions and Studies of the Cooperative Effect Between Cationic Surfactant and Acid Counterions. *Journal of Bio- and Tribo-Corrosion* **2018**, *4*, https://doi.org/10.1007/s40735-018-0127-2.

43.   Ardakani, E.K.; Kowsari, E.; Ehsani, A. Imidazolium derived polymeric ionic liquid as a green inhibitor for corrosion inhibition of mild steel in 1.0 M HCl: Experimental and computational study. *Colloids and Surfaces A: Physicochemical and Engineering Aspects* **2020**, *586*, https://doi.org/10.1016/j.colsurfa.2019.124195.

44.   Gece, G.; Bilgiç, S. Quantum chemical study of some cyclic nitrogen compounds as corrosion inhibitors of steel in NaCl media. *Corrosion Science* **2009**, *51*, 1876-1878, https://doi.org/10.1016/j.corsci.2009.04.003.

45.   Roque, J.M.; Pandiyan, T.; Cruz, J.; García-Ochoa, E. DFT and electrochemical studies of tris(benzimidazole-2-ylmethyl)amine as an efficient corrosion inhibitor for carbon steel surface. *Corrosion Science* **2008**, *50*, 614-624, https://doi.org/10.1016/j.corsci.2007.11.012.

46.   Hegazy, M.A. Novel cationic surfactant based on triazole as a corrosion inhibitor for carbon steel in phosphoric acid produced by dihydrate wet process. *Journal of Molecular Liquids* **2015**, *208*, 227-236, https://doi.org/10.1016/j.molliq.2015.04.042.